A heterozygous missense *SCN5A* mutation associated with early repolarization syndrome

NING LI[1], RONGRONG WANG[1], CUIHONG HOU[2], YINHUI ZHANG[1], SIYONG TENG[2] and JIELIN PU[1,2]

[1]State Key Laboratory of Cardiovascular Disease and [2]Center for Arrhythmia Diagnosis and Treatment, National Center for Cardiovascular Diseases, Fuwai Hospital, Chinese Academy of Medical Sciences and Peking Union Medical College, Beijing, P.R. China

Received July 2, 2012; Accepted September 10, 2012

DOI: 10.3892/ijmm.2013.1422

Abstract. The genetic background of early repolarization syndrome (ERS) has not been fully understood. In this study, we identified a missense *SCN5A* mutation and a polymorphism in a patient with ERS and characterized the functional consequences of the two variants. The functional consequences of mutant channels were investigated with the patch-clamp technique, immunocytochemical studies and real-time PCR. A 19-year-old female proband with recurrent syncope had a documented electrocardiogram with ventricular fibrillation (VF) proceeded by large J waves in leads I, II, III, aVF and V_2-V_6. Genetic analysis revealed that the patient carried a missense mutation of c.4297 G>C and a synonymous polymorphism of T5457C on the same allele of the *SCN5A* gene. Patch-clamp experiments demonstrated that the c.4297 G>C mutation significantly reduced the sodium current (I_{Na}) density and altered the channel kinetics. Immunocytochemical studies demonstrated that the mutation dramatically inhibited the expression of sodium channels in the cell membrane and in the cytoplasm, although the mRNA levels remained in the normal range. Noteworthy, the reduction in I_{Na} density may be partially restored from the co-existence of the T5457C polymorphism on the same allele by the upregulation of mRNA levels. In conclusion, our study indicated that the c.4297 G>C mutation caused the 'loss-of-function' of sodium channels that may account for the clinical phenotype of ERS. The reduction in I_{Na} density was due to a decreased number of sodium channels caused by abnormal translation processes. The T5457C polymorphism partially rescued the I_{Na} density of the mutant channels by the upregulation of mRNA levels.

Correspondence to: Professor Jielin Pu, Pathology and Physiology Research Center and Center for Arrhythmia Diagnosis and Treatment, National Center for Cardiovascular Diseases, Fuwai Hospital, Chinese Academy of Medical Sciences and Peking Union Medical College, 167 Bei-Li-Shi Road, Xi-Cheng, Beijing 100037, P.R. China
E-mail: jielinpu@yahoo.com

Abbreviations: VF, ventricular fibrillation; ERS, early repolarization syndrome; BrS, Brugada syndrome; SNP, single nucleotide polymorphism; WT, wild-type; HEK293, human embryonic kidney 293 cells; I_{Na}, sodium current; I_{to}, transient outward current

Key words: early repolarization, ventricular fibrillation, sudden death, genetics, SCN5A

Introduction

The early repolarization pattern consisting of a J-point elevation, notching or slurring of the terminal portion of the R wave (J wave) and tall/symmetric T wave is a common finding on the electrocardiography (ECG) in young healthy men or athletes and is considered a 'benign' ECG manifestation for a long period of time (1-3). However, recent evidence has demonstrated that early repolarization may be associated with an increased risk for ventricular fibrillation (VF), depending on the locations and magnitude of the J wave and ST-segment elevation (4,5). Thus, Antzelevitch and Yan (1) proposed a new conceptual framework, inherited J wave syndromes, to describe the arrhythmic phenotypes. Inherited J wave syndromes, as a continuous spectrum of arrhythmic phenotypes, has been divided into four different subtypes in terms of anatomical locations of J wave and ST-segment elevation and clinical consequences, including early repolarization in the lateral precordial leads [early repolarization syndrome (ERS) type 1], in the inferior or inferolateral leads (ERS type 2), globally in the inferior, lateral and right precordial leads (ERS type 3) and in the right precordial leads [Brugada syndrome (BrS)] (1). However, the genetic basis of the three types of ERS has not been well defined. To date, 'loss-of-function' mutations in the *CACNA1C*, *CACNB2* and *CACNA2D1* genes and 'gain-of-function' mutations in the *KCNJ8* gene have been identified in patients with ERS (6-8).

In the present study, we described an unreported missense mutation of c.4297 G>C in the *SCN5A* gene, which encoded the α subunit of the cardiac voltage-gated sodium channel Nav1.5, leading to prominent J waves and ST-segment elevation in the inferior, lateral and precordial leads accompanied with VF in a female proband. We identified an unpublished synonymous single nucleotide polymorphism (SNP) of T5457C in the *SCN5A* gene in the proband, her mother and sister. We characterized the functional consequences of the mutation as well as the interaction between the mutation and the SNP.

Materials and methods

Clinical examination. The proband and her first-degree relatives underwent clinical evaluation, including medical history, physical examination and 12-lead ECG and echocardiographic examinations (Figs. 1 and 2). The study conformed to the principles outlined in the Declaration of Helsinki. The institutional ethics committee approved all the research protocols and written informed consents were obtained from all participants.

Genotyping. Genomic DNA was isolated from peripheral blood leukocytes using a TIANamp Blood DNA isolation kit (Tiangen, Beijing, China) according to the manufacturer's instructions. All exons of the *SCN5A*, *KCND3*, *CACNA1C*, *CACNB2*, *KCNE3*, *SCN1B* and *KCNJ8* genes were amplified by polymerase chain reaction (PCR) and were analyzed by direct sequencing. Whenever the variant was discovered in the proband or her family members, it would be confirmed in 500 unrelated healthy Chinese individuals (1,000 reference alleles) to determine the distinction between mutation and polymorphism.

Mutagenesis and expression studies. The technique for site-directed mutagenesis and wild-type (WT)-SCN5A plasmid were prepared in our laboratory (9). Three mutations based on the genotypes of the patient and her family (c.4297 G>C -SCN5A, T5457C-SCN5A and c.4297 G>C-T5457C-SCN5A) were created on the WT-SCN5A background (GenBank ID: NM198056). All mutations were verified by sequencing and then subcloned back into the pcDNA3.1 vector. The heterologous expression was performed as previously described (9). Briefly, the human embryonic kidney (HEK) 293 cells were transiently transfected with 0.6 μg cDNA (detailed composition is shown in Table I) using an Effectene Transfection Reagent (Qiagen, Hilden, Germany) according to the manufacturer's protocol. Green fluorescent protein gene (0.2 μg) was cotransfected as an indicator. The transfected cells were cultured for 36 h before sodium current (I_{Na}) was recorded. More than 3 independent experiments were conducted to confirm the reproducibility of the results.

Patch-clamping. I_{Na} was measured using whole-cell configuration of the patch-clamp technique as previously described (10) with Axonpatch 700B amplifiers (Axon Instruments, Foster City, CA, USA). The resistance of pipettes in the bath solution ranged from 1.5 to 2 MΩ. For whole-cell recording, the internal pipette solution contained (in mmol/l) CsF 120, CsCl 20, ethylene glycol tetraacetic acid 2.0, $MgCl_2$ 1.0 and HEPES 5 (pH 7.4). The bath solution contained (in mmol/l) NaCl 30, CsCl 110, $CaCl_2$ 1.8, $MgCl_2$ 1.0 and HEPES 10 (pH 7.4). No leak subtraction was applied during recording. All measurements were obtained at room temperature (20-22˚C).

RNA isolation and quantitative real-time PCR. Total RNA was extracted from transfected HEK293 cells using TRIzol reagent (Invitrogen Life Technologies, Carlsbad, CA, USA) according to the manufacturer's instructions. The concentration of RNA was determined by the UV Visible spectrophotometer and 1 μg total RNA was subsequently reverse-transcribed to cDNA using Moloney murine leukemia virus reverse transcriptase (Promega Corporation, Madison, WI, USA). Quantitative real-time PCR (11) was performed on an ABI 7300 real-time PCR instrument (Applied Biosystems, Foster City, CA, USA) with the *GAPDH* gene, whose expression is very stable in HEK293 cells, as an internal control for data normalization. The primers were as follows: forward, 5'-GAGATGCTGCAGGTCGGAAAC-3' and reverse, 5'-GATGACGATGATGCTGTCGAAGA-3'. The PCR cycles consisted of denaturation at 95˚C for 15 sec, annealing and extension at 60˚C for 1 min for 40 cycles. Each sample was analyzed 3 times. The $2^{-\triangle\triangle Ct}$ method was used to analyze the relative expression of protein.

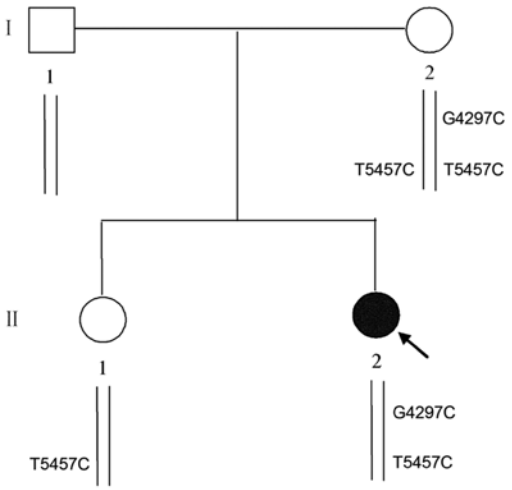

Figure 1. Pedigree of the family. Squares and circles represent male and female members, respectively. Solid circle (arrow) represents the proband carrying a heterozygous G4297C mutation and a heterozygous T5457C polymorphism in the *SCN5A* gene. The individual I-2 is asymptomatic despite carrying the G4297C mutation. Moreover, she also has a homozygous T5457C polymorphism.

Immunocytochemistry. Immunocytochemical experiments were performed as previously described (12). Briefly, cells were fixed, blocked and incubated with mouse monoclonal to Nav1.5 IgM primary antibody (1:40 dilution) (Abcam, Cambridge, UK) overnight at 4˚C. The cells were then incubated in anti-mouse FITC-conjugated donkey secondary antibody (1:500 dilution) (Jackson ImmunoResearch, West Grove, PA, USA) for 1 h at room temperature in the dark. Confocal images were obtained using a confocal laser scanning microscope (Leica TCS SP2; Leica, Wetzlar, Germany) and were analyzed with NIH image software (Image J).

Statistical analysis. Data are represented as the means ± standard error of the mean (SEM). Student's t-test analysis was performed for the comparison of two means, while one-way ANOVA was performed for comparisons of multiple means using statistical software SPSS 13.0. A value of $P<0.05$ was considered to indicate a statistically significant difference.

Results

Clinical manifestation and genotyping. The proband, a 19-year-old female was admitted to the Fu Wai Hospital

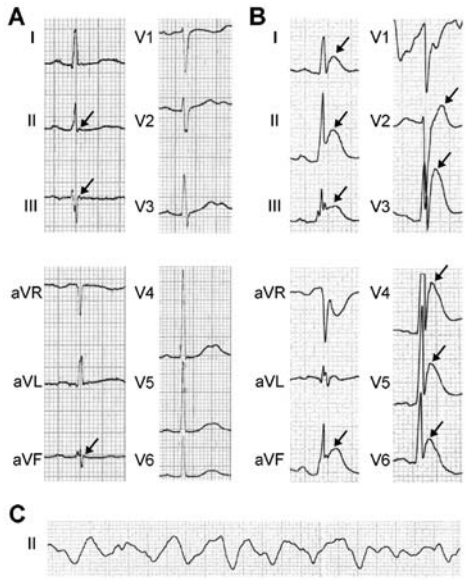

Figure 2. 12-Lead ECG recordings of the proband. (A) The baseline ECG demonstrates tiny, hump-like J waves (arrows) in the inferior leads and a borderline prolongation of the PR interval (200 msec). The RR interval was 1,095 msec. (B) Prominent J waves and ST-segment elevation (arrows) are present in ECG leads I, II, III, aVF and V_2-V_6 before VF occurred. RR interval was 585 msec. (C) A spontaneous onset of VF. VF, ventricular fibrillation.

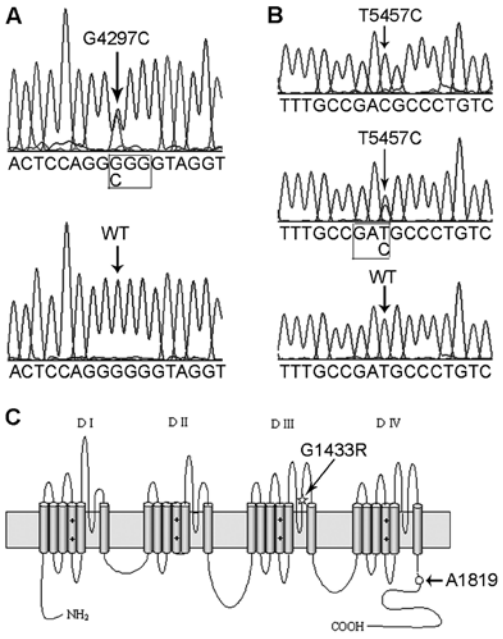

Figure 3. DNA sequence analysis and schematic representation of the α subunit of the sodium channel. (A) DNA sequence analysis of the proband demonstrated a G to C mutation of the *SCN5A* gene at position 4297 leading to a glycine to arginine substitution at position 1433 of the α subunit of the sodium channel. (B) DNA sequence analysis of the proband and her mother demonstrated a T to C substitution of the *SCN5A* gene at position 5457 resulting in a silent polymorphism at position 1819 of the α subunit of the sodium channel. (C) The α subunit of the sodium channel, a transmembrane protein with four domains, indicates the location of the 1433 amino acid residue, whereas it denotes the common polymorphism that is located in the 1819 amino acid residue.

(Beijing, China) due to a history of recurrent syncope at rest (a total of 4 times since the age of 16). The ECG that was obtained at the emergency department exhibited prominent

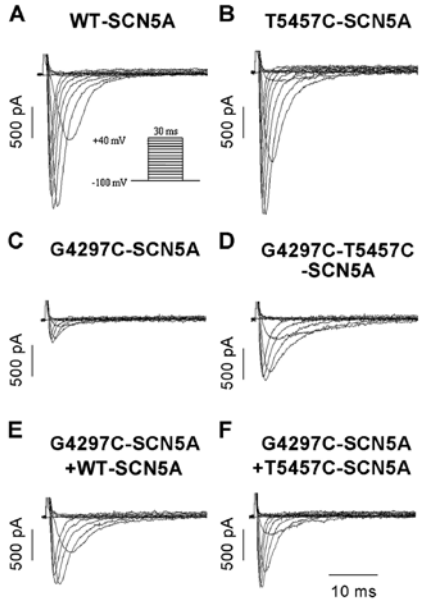

Figure 4. The representative sodium current (I_{NA}) traces recorded from HEK293 cells transfected transiently with (A) WT-SCN5A, (B) T5457C-SCN5A, (C) 4297C-SCN5A, (D) G4297C-T5457C-SCN5A, (E) G4297C-SCN5A + WT-SCN5A or (F) G4297C-SCN5A + T5457C-SCN5A.

J waves and ST-segment elevation in leads I, II, III, aVF and V_2-V_6 (Fig. 2B) before VF occurred (Fig. 2C). Subsequently, the VF episode was terminated by cardioversion. There was no difference in clinical state that may explain the marked J waves and ST-segment elevation in the documented ECG. Myocardial infarction was excluded by cardiac enzyme tests and coronary angiography. The routine echocardiography demonstrated a structural and functional normal heart. The baseline ECG was within normal limits with the exception of tiny, hump-like J waves in the inferior leads and a borderline prolongation of the PR interval (200 msec) (Fig. 2A). The amplitude of ST-segment elevation fluctuated from day to day. Programmed electrical stimulation induced VF that was converted to sinus rhythm by cardioversion. Since the sodium channel blockers, such as ajmaline, flecainide and procainamide, were not available in China, drug challenge was not performed. According to the clinical manifestations, ERS type 3 was diagnosed and an implantable cardioverter defibrillator was implanted with the pacing rate programmed to 60 bpm. After amiodarone (200 mg/day) and metoprolol (50 mg/day) administration, the proband remained symptom-free for a period of 18 months. However, in the nineteenth month, the patient was shocked due to a VF episode with a heart rate >260 bpm. All family members lived asymptomatic and there was no family history of sudden death.

A heterozygous missense mutation of c.4297 G>C, located in exon 24 of the *SCN5A* gene, was identified in the proband using direct DNA sequencing (Fig. 3A). The mutation led to a substitution of an arginine for a glycine at position 1433 that was predicted to be in the extracellular loop between the pore region and the S6 transmembrane segment in the domain III of the α subunit of the sodium channels (Fig. 3C). The c.4297 G>C mutation was also detected in her mother but not in 500 unrelated healthy subjects. In addition, a heterozygous SNP, T5457C, which is located in exon 28 of the *SCN5A*

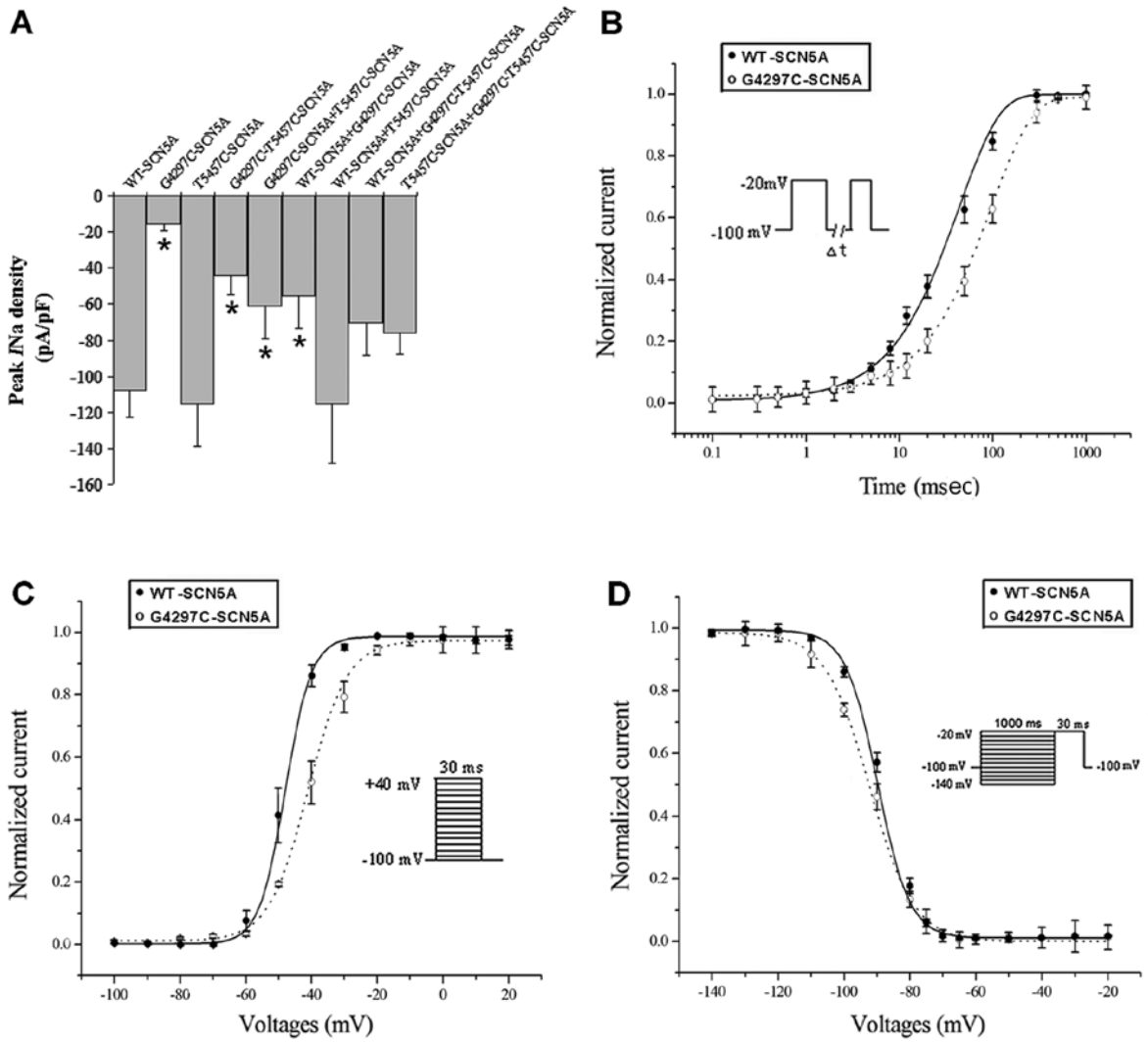

Figure 5. Peak I_{Na} densities and channel kinetics. (A) The I_{Na} densities of WT, T5457C SNP and WT + T5457C SNP were similar (P>0.05). The T5457C SNP slightly increased the current density, while the G4297C mutation significantly reduced I_{Na} to 14.63% of the WT current (P<0.05). The I_{Na} densities of the cells transfected with G4297C-T5457C-SCN5A or cotransfected with G4297C and T5457C or WT-SCN5A were all significantly increased compared to that of cells transfected with the G4297C mutant alone (P<0.05). In the heterozygous expression system, the coexpression of G4297C-T5457C-SCN5A with WT-SCN5A (as the nature of the proband) or with T5457C-SCN5A (as the nature of her mother) increased the I_{Na} up to 65 or 70% compared to the WT channels. (B) Recovery from inactivation was slower in the G4297C mutant compared to that in the WT channels. (C) The G4297C mutation shifted the steady-state activation curve to a more positive potential, while (D) it had no effect on the steady-state inactivation. *Significant difference from the WT control, P<0.05.

gene, was discovered in the proband; however, the T5457C polymorphism did not cause a change in the protein sequence (Fig. 3B and C). Genetic analysis revealed that her mother carried a homozygous T5457C polymorphism and her sister carried a heterozygous T5457C polymorphism, while her farther carried no such variants (Fig. 1). Since the substitution of C for T occurred at a frequency of 42.67% within a population including 500 unrelated healthy subjects, we confirmed that the T5457C variant was a polymorphism. Moreover, no other mutations or variants were discovered in the screened genes in the proband and the family.

Electrophysiology of G4297C and T5457C channels. I_{Na} was recorded from the HEK293 cells transiently transfected with the WT-SCN5A, G4297C-SCN5A or T5457C-SCN5A plasmid using the whole-cell configuration of the patch-clamp technique. The G4297C mutation dramatically reduced I_{Na} density (-107.65±14.70 pA/pF in WT, n=8 vs. -15.75±3.72 pA/pF in the mutant, n=12, P<0.05) (Fig. 4A and C) and shifted the steady-state activation curve to a more positive potential compared with the WT channels (P<0.05) (Fig. 5C and Table I). By contrast, the mutation had no effect on the steady-state inactivation (Fig. 5D and Table I), although it inhibited the recovery from inactivation (P<0.05) (Fig. 5B and Table I).

The T5457C variant was a relative benign polymorphism since it did not change the current density (-115.47±23.25 pA/pF, n=8, P>0.05) (Fig. 4B), steady-state activation and steady-state inactivation of the sodium channels, although it prolonged the recovery from inactivation compared with the WT channels (P<0.05) (Table I).

Rescue effect of the T5457C polymorphism on G4297C mutant channels. Furthermore, we characterized the interaction between the G4297C mutation and the T5457C polymorphism. Inserting the T5457C polymorphism into the G4297C

Table I. Average values of activation, inactivation and recovery from inactivation parameters.

Channels	N	Steady-state activation		Steady-state inactivation		Recovery from inactivation		
		$V_{1/2}$, mV	k	$V_{1/2}$, mV	k	τ_f, msec	τ_s, msec	A_f
WT-SCN5A (0.6 μg)	8	-50.72±1.46	3.61±0.32	-88.61±0.78	5.28±0.14	24.25±4.26	189.94±14.56	0.70±0.01
G4297C-SCN5A (0.6 μg)	9	-39.07±1.80[a]	6.18±0.36[a]	-91.39±1.95	4.79±0.47	66.01±4.94[a]	257.99±8.84[a]	0.54±0.01[a]
T5457C-SCN5A (0.6 μg)	8	-47.26±2.34	4.50±0.54	-90.91±1.00	5.35±0.17	29.38±3.44	248.93±6.95[a]	0.50±0.02[a]
G4297C-T5457C-SCN5A (0.6 μg)	8	-40.78±2.19[a]	5.29±0.35[a]	-85.71±1.96	4.78±0.31	56.46±2.48[a]	244.10±9.11[a]	0.52±0.01[a]
G4297C-SCN5A + T5457C-SCN5A (0.3 + 0.3 μg)	7	-39.10±2.69[a]	5.46±0.42[a]	-88.64±0.86	5.03±0.25	46.43±4.36[a]	232.85±10.55[a]	0.50±0.01[a]
WT-SCN5A + G4297C-SCN5A (0.3 + 0.3 μg)	5	-46.01±2.57	4.91±0.68	-87.56±0.98	5.55±0.16	25.92±4.20	204.75±9.81	0.69±0.01
WT-SCN5A + T5457C-SCN5A (0.3 + 0.3 μg)	5	-47.87±3.13	3.99±1.80	-87.97±1.99	5.36±0.27	27.43±3.65	258.76±12.74[a]	0.56±0.02[a]
WT-SCN5A + G4297C-T5457C-SCN5A (0.3 + 0.3 μg)	9	-42.60±1.77[a]	5.31±0.44[a]	-85.21±1.53	5.09±0.27	47.05±6.09[a]	236.03±10.13[a]	0.49±0.02[a]
T5457C-SCN5A + G4297C-T5457C-SCN5A (0.3 + 0.3 μg)	5	-43.72±2.51[a]	4.89±0.43[a]	-88.67±2.94	5.66±0.30	51.47±7.14[a]	252.87±13.82[a]	0.51±0.01[a]

The kinetic data are represented as the means ± SEM. $V_{1/2}$ indicates the voltage at which 50% of the channels were activated or inactivated, and k indicates the slope factor. τ_f, τ_s and A_f represent the fast time constant, the slow time constant, and the fractional amplitude of fast recovery components, respectively. [a]Significant difference from WT control, P<0.05.

Figure 6. Confocal imaging of WT and mutant channels. (A) The background fluorescence of the non-transfected cells. Blue fluorescence indicates the nuclei. (B) The peripheral localization of fluorescence in cells transfected with WT-SCN5A. (C) Less fluorescence in the cell membrane and cytoplasm was detected in cells transfected with G4297C-SCN5A. (D) In the cells transfected with G4297C-T5457C-SCN5A, the membrane sodium channel proteins were significantly increased compared with the G4297C-SCN5A group. The calibration bar, 20 μm. (E) Summary data demonstrated that the membrane to intracellular fluorescence ratio in the G4297C group was markedly reduced compared to that in the WT group; however, the ratio significantly increased in the G4297C-T5457C group compared with the G4297C group. *P<0.05 represents a significant difference from the WT control, #P<0.05 represents a significant difference from the G4297C group; n=10 in each group.

mutant construct (G4297C-T5457C-SCN5A) partially restored the I_{Na} density (-44.12±10.45 pA/pF, n=8) (P<0.05, Fig. 4D) but without having an effect on mutant channel kinetics compared with the G4297C channels (Table I). However, coexpression of the T5457C polymorphism and G4297C mutation on separate constructs had no significant effect on the I_{Na} density of mutant channels, since the similar current densities were recorded from cells coexpressing G4297C-SCN5A and WT or T5457C-SCN5A (-55.66±18.01 pA/pF, n=7 vs. -61.02±17.80 pA/pF, n=5, P>0.05) (Fig. 4E and F). Additionally, we expressed the cDNA constructs to simulate the distribution patterns of G4297C and T5457C in the proband and her family. Coexpression of G4297C-T5457C-SCN5A with WT-SCN5A (as the nature of the proband) or G4297C-T5457C-SCN5A with T5457C-SCN5A (as the nature of her mother) increased the I_{Na} up to 65 or 70% in the WT channels. The peak current densities are plotted in Fig. 5A for all combinations of WT-SCN5A, G4297C-SCN5A, T5457C-SCN5A and G4297C-T5457C-SCN5A constructs.

Transcription of WT and mutant cDNAs. Quantitative real-time PCR was used to detect the WT and mutant mRNA levels. The mRNA of SCN5A was not detected in the non-transfected cells. There was no significant difference in mRNA levels between cells transfected with WT-SCN5A and the G4297C mutant (P>0.05). The mRNA level of G4297C-T5457C-SCN5A was increased by 6-fold compared to that of WT-SCN5A (P<0.05).

Confocal imaging. To investigate the cellular localization of the WT and mutant channels, immunocytochemical experiments were performed. The non-transfected cells displayed background fluorescence (Fig. 6A). As expected, the periphery localization was exhibited in cells with WT channels (Fig. 6B). By contrast, cells transfected with G4297C mutant channels displayed a very low expression both in the cell membrane and in the cytoplasm (Fig. 6C). However, the G4297C-T5457C channels demonstrated a significantly higher expression with a peripheral localization pattern compared to that of the G4297C channels, consistent with the increased mRNA levels of G4297C-T5457C-SCN5A compared with the G4297C channels, which indicated that the T5457C polymorphism partially rescued the expression of G4297C mutant channels (Fig. 6D). Summary data depicted in Fig. 6E revealed that the average fluorescence intensity per unit area in the membrane divided by the average fluorescence intensity per unit area in intracellular compartments (membrane to intracellular fluorescence ratio) was markedly reduced in the G4297C group compared to that in the WT group (P=0.0007); however, the ratio significantly increased in the G4297C-T5457C group compared with the G4297C group (P=0.017) (n=10 for all groups).

Discussion

In this study, we identified an unreported *SCN5A* mutation G4297C in a young female patient with idiopathic VF followed by J waves and ST-segment elevation in the inferior, lateral and precordial leads demonstrated by documented ECG. According to the clinical manifestation of the lack of typical Brugada waves in the right precordial V_1 lead, the patient was not diagnosed as BrS (13,14). Recently, a multicenter study revealed that J wave and ST-segment elevation in the inferior or lateral leads, also termed as early repolarization (15,16), accounted for 31% of 206 patients with idiopathic VF (4). It has also been reported that up to 11% of patients with BrS presented J wave and ST-segment elevation in the inferior-lateral leads associated with an increased number of symptoms (5). Therefore, the nomenclature of ERS or BrS remains unclear. Based on the new conceptual framework proposed by Antzelevitch and Yan (1), our patient may be diagnosed as ERS type 3.

In the present study, we reported a missense G4297C mutation in the *SCN5A* gene. After excluding variants in other genes associated with ERS (6-8) and BrS (17), including *KCND3*, *CACNA1C*, *CACNB2*, *KCNE3*, *SCN1B* and *KCNJ8*, we speculated that the G4297C mutation in the *SCN5A* gene was the causative mutation. The patch-clamp study demonstrated that the G4297C mutation caused a significant decrease in I_{Na} density as well as altered biophysical characteristics of sodium channels such as prolonged recovery time from inactivation and depolarizing shift in activation. The altered properties predisposed the sodium channels to a 'loss-of-function'. Further study demonstrated that the mRNA levels of WT and G4297C mutant channels were similar. However, immunocytochemistry demonstrated that the G4297C mutant channels displayed a very low expression both in the cell membrane and in the cytoplasm. The result suggests that G4297C does not cause a trafficking defect (18), in contrast, it affects the translation process or degradation of the mutant protein. This mechanism differs from three well-known primary mechanisms that cause a 'loss-of-function' of sodium channels such as i) formation of nonfunctional channels; ii) altered gating properties; and iii) defective trafficking (18,19). Thus, our findings may represent a novel mechanism for the 'loss-of-function' of sodium channels.

Moreover, several studies found that the R282H mutation in the *SCN5A* gene, which leads to BrS, may be fully rescued by the H558R polymorphism that restores the trafficking of the mutant protein (20,21). The rescue effect of the synonymous polymorphism T5457C identified in our study has not yet been investigated. Our study demonstrated that T5457C did partially restore the G4297C mutant channels based on the fact that the mRNA level of the G4297C-T5457C-SCN5A mutant significantly increased compared to that of the G4297C mutant, corresponding to a concomitant proportional increase in the number of sodium channels on the cell surface. A similar phenomenon has been observed in the *ABCC2* gene that encodes the multidrug resistance-associated protein 2 (MRP2). The synonymous C1146G SNP in the *ABCC2* gene increased MRP2 mRNA expression by 2-fold in human livers (22). However, the essential mechanism by which a synonymous SNP increases mRNA expression remains unclear. Several studies have focused on the possibility that the synonymous SNP alters the stability of mRNA, a phenomenon suggested by the synonymous C3435T SNP in the *ABCB1* gene, encoding multidrug resistance polypeptide 1 and the synonymous C971T SNP in the *CDSN* gene encoding corneodesmosin (23,24). Another explanation was that the SNP may be in linkage disequilibrium with other polymorphism(s) acting at the transcriptional level (22).

At present, the transmural voltage gradient mediated by the transient outward current (I_{to}) during the early repolarization phase has been accepted as an explanation of the pathophysiological mechanism of J wave or ST-segment elevation on the ECG when the corresponding inward I_{Na} was reduced (25). I_{to} was often more prominent in the epicardium of the right ventricle compared to that of the left ventricle (26), and therefore, ST-segment elevation was predisposed to localizing in the right precordial leads, as noted in BrS. By contrast, in our study, the J waves and ST-segment elevation of the proband were confined to the inferior, lateral and left precordial leads. The possible explanation may be associated with the gender-related difference in I_{to} distribution. In the human ventricle, the transmural I_{to} gradient is formed by the differential expression of *KChIP2*, the gene encoding the β subunit of the I_{to} (27). The expression of *KChIP2* gene is negatively regulated via the homeodomain Iroquois transcription factor *IRX5* and *IRX3* (28). Recently, Gaborit *et al* (28) provided evidence that the expression of *KChIP2* is increased in the female left ventricle, consistent with the decreased expression of *IRX3* and *IRX5* compared with the

right ventricle. The distinction of expression levels of *KChIP2*, *IRX3* and *IRX5* between male and female hearts may cause the J waves and ST-segment elevation in the inferior, lateral and left precordial leads in female patients as noted in our proband.

We reported a missense mutation of G4297C in the *SCN5A* gene, which caused the 'loss-of-function' of sodium channels, leading to the clinical phenotype of ERS type 3. Our findings may represent a novel mechanism for the 'loss-of-function' of sodium channels by decreasing the number of sodium channels due to abnormal translation processes. The synonymous T5457C polymorphism may partially restore the function of the G4297C mutant channels through the upregulation of mRNA levels. However, several limitations existed in this study. First, the reasons for incomplete penetrance in patient I-2 depicted in Fig. 1 were not elucidated. Second, although the probability was very low, it was unclear whether the reported mutation and the SNP were on the same allele. The reason why the T5457C SNP prolonged the recovery from the inactivation of the sodium channels requires further investigation.

Acknowledgements

The National Basic Research Program of China (973 program, 2007CB512000 and 2007CB512008) provided support to J. Pu for this research.

References

1. Antzelevitch C and Yan GX: J wave syndromes. Heart Rhythm 7: 549-558, 2010.
2. Miyazaki S, Shah AJ and Haïssaguerre M: Early repolarization syndrome - a new electrical disorder associated with sudden cardiac death. Circ J 74: 2039-2044, 2010.
3. Yan GX, Lankipalli RS, Burke JF, Musco S and Kowey PR: Ventricular repolarization components on the electrocardiogram: cellular basis and clinical significance. J Am Coll Cardiol 42: 401-409, 2003.
4. Haïssaguerre M, Derval N, Sacher F, Jesel L, Deisenhofer I, de Roy L, Pasquié JL, Nogami A, Babuty D, Yli-Mayry S, *et al*: Sudden cardiac arrest associated with early repolarization. N Engl J Med 358: 2016-2023, 2008.
5. Sarkozy A, Chierchia GB, Paparella G, Boussy T, De Asmundis C, Roos M, Henkens S, Kaufman L, Buyl R, Brugada R, *et al*: Inferior and lateral electrocardiographic repolarization abnormalities in Brugada syndrome. Circ Arrhythm Electrophysiol 2: 154-161, 2009.
6. Haïssaguerre M, Chatel S, Sacher F, Weerasooriya R, Probst V, Loussouarn G, Horlitz M, Liersch R, Schulze-Bahr E, Wilde A, *et al*: Ventricular fibrillation with prominent early repolarization associated with a rare variant of KCNJ8/KATP channel. J Cardiovasc Electrophysiol 20: 93-98, 2009.
7. Medeiros-Domingo A, Tan BH, Crotti L, Tester DJ, Eckhardt L, Cuoretti A, Kroboth SL, Song C, Zhou Q, Kopp D, *et al*: Gain-of-function mutation, S422L, in the KCNJ8-encoded cardiac K(ATP) channel Kir6.1 as a pathogenic substrate for J-wave syndromes. Heart Rhythm 7: 1466-1471, 2010.
8. Burashnikov E, Pfeiffer R, Barajas-Martinez H, Delpón E, Hu D, Desai M, Borggrefe M, Häissaguerre M, Kanter R, Pollevick GD, *et al*: Mutations in the cardiac L-type calcium channel associated with inherited J-wave syndromes and sudden cardiac death. Heart Rhythm 7: 1872-1882, 2010.
9. Teng S, Gao L, Paajanen V, Pu J and Fan Z: Readthrough of nonsense mutation W822X in the SCN5A gene can effectively restore expression of cardiac Na^+ channels. Cardiovasc Res 83: 473-480, 2009.
10. Hamill OP, Marty A, Neher E, Sakmann B and Sigworth FJ: Improved patch-clamp techniques for high-resolution current recording from cells and cell-free membrane patches. Pflugers Arch 391: 85-100, 1981.
11. Okada T, Ding G, Sonoda H, Kajimoto T, Haga Y, Khosrowbeygi A, Gao S, Miwa N, Jahangeer S and Nakamura S: Involvement of N-terminal-extended form of sphingosine kinase 2 in serum-dependent regulation of cell proliferation and apoptosis. J Biol Chem 280: 36318-36325, 2005.
12. Yao Y, Teng S, Li N, Zhang Y, Boyden PA and Pu J: Aminoglycoside antibiotics restore functional expression of truncated HERG channels produced by nonsense mutations. Heart Rhythm 6: 553-560, 2009.
13. Wilde AA, Antzelevitch C, Borggrefe M, Brugada J, Brugada R, Brugada P, Corrado D, Hauer RN, Kass RS, Nademanee K, *et al*: Study Group on the Molecular Basis of Arrhythmias of the European Society of Cardiology: Proposed diagnostic criteria for the Brugada syndrome: consensus report. Circulation 106: 2514-2519, 2002.
14. Antzelevitch C, Brugada P, Borggrefe M, Brugada J, Brugada R, Corrado D, Gussak I, LeMarec H, Nademanee K, Perez Riera AR, *et al*: Brugada syndrome: report of the second consensus conference: endorsed by the Heart Rhythm Society and the European Heart Rhythm Association. Circulation 111: 659-670, 2005.
15. Shu J, Zhu T, Yang L, Cui C and Yan GX: ST-segment elevation in the early repolarization syndrome, idiopathic ventricular fibrillation, and the Brugada syndrome: cellular and clinical linkage. J Electrocardiol 38 (Suppl 4): S26-S32, 2005.
16. Di Grande A, Tabita V, Lizzio MM, Giuffrida C, Bellanuova I, Lisi M, Le Moli C and Amico S: Early repolarization syndrome and Brugada syndrome: is there any linkage? Eur J Intern Med 19: 236-240, 2008.
17. Hedley PL, Jørgensen P, Schlamowitz S, Moolman-Smook J, Kanters JK, Corfield VA and Christiansen M: The genetic basis of Brugada syndrome: a mutation update. Hum Mutat 30: 1256-1266, 2009.
18. Baroudi G, Pouliot V, Denjoy I, Guicheney P, Shrier A and Chahine M: Novel mechanism for Brugada syndrome: defective surface localization of an SCN5A mutant (R1432G). Circ Res 88: E78-E83, 2001.
19. Baroudi G, Acharfi S, Larouche C and Chahine M: Expression and intracellular localization of an SCN5A double mutant R1232W/T1620M implicated in Brugada syndrome. Circ Res 90: E11-E16, 2002.
20. Poelzing S, Forleo C, Samodell M, Dudash L, Sorrentino S, Anaclerio M, Troccoli R, Iacoviello M, Romito R, Guida P, *et al*: SCN5A polymorphism restores trafficking of a Brugada syndrome mutation on a separate gene. Circulation 114: 368-376, 2006.
21. Gui J, Wang T, Trump D, Zimmer T and Lei M: Mutation-specific effects of polymorphism H558R in SCN5A-related sick sinus syndrome. J Cardiovasc Electrophysiol 21: 564-573, 2010.
22. Niemi M, Arnold KA, Backman JT, Pasanen MK, Gödtel-Armbrust U, Wojnowski L, Zanger UM, Neuvonen PJ, Eichelbaum M, Kivistö KT and Lang T: Association of genetic polymorphism in ABCC2 with hepatic multidrug resistance-associated protein 2 expression and pravastatin pharmacokinetics. Pharmacogenet Genomics 16: 801-808, 2006.
23. Wang D, Johnson AD, Papp AC, Kroetz DL and Sadée W: Multidrug resistance polypeptide 1 (MDR1, ABCB1) variant 3435C>T affects mRNA stability. Pharmacogenet Genomics 15: 693-704, 2005.
24. Capon F, Allen MH, Ameen M, Burden AD, Tillman D, Barker JN and Trembath RC: A synonymous SNP of the corneodesmosin gene leads to increased mRNA stability and demonstrates association with psoriasis across diverse ethnic groups. Hum Mol Genet 13: 2361-2368, 2004.
25. Yan GX and Antzelevitch C: Cellular basis for the Brugada syndrome and other mechanisms of arrhythmogenesis associated with ST-segment elevation. Circulation 100: 1660-1666, 1999.
26. Di Diego JM, Cordeiro JM, Goodrow RJ, Fish JM, Zygmunt AC, Pérez GJ, Scornik FS and Antzelevitch C: Ionic and cellular basis for the predominance of the Brugada syndrome phenotype in males. Circulation 106: 2004-2011, 2002.
27. Rosati B, Pan Z, Lypen S, Wang HS, Cohen I, Dixon JE and McKinnon D: Regulation of KChIP2 potassium channel beta subunit gene expression underlies the gradient of transient outward current in canine and human ventricle. J Physiol 533: 119-125, 2001.
28. Gaborit N, Varro A, Le Bouter S, Szuts V, Escande D, Nattel S and Demolombe S: Gender-related differences in ion-channel and transporter subunit expression in non-diseased human hearts. J Mol Cell Cardiol 49: 639-646, 2010.